Stress intensity factors of the rib-to-deck welded joint at the crossbeam conjunction in OSDs

Wu, Weijian; Kolstein, Henk; Veljkovic, Milan

DOI
10.1016/j.prostr.2018.12.214

Publication date
2018

Document Version
Final published version

Published in
Procedia Structural Integrity

Available online at www.sciencedirect.com

ScienceDirect

Procedia Structural Integrity 13 (2018) 2017–2023

Structural Integrity Procedia

www.elsevier.com/locate/procedia

ECF22 - Loading and Environmental effects on Structural Integrity

Stress intensity factors of the rib-to-deck welded joint at the crossbeam conjunction in OSDs

Weijian Wu[a,*], Henk Kolstein[a], Milan Veljkovic[a]

[a]*Faculty of Geoscience and Engineering, Delft University of Technology, Delft 2628 CN, Netherlands*

Abstract

The orthotropic steel decks (OSDs) are one of the most widely used bridge components, especially in moveable and long span bridges. Numerous cracks have been detected in this type of deck in existing bridges, mainly in the welded joints. The fatigue performance of the bridge deck dominates its design. Among them, the crack at the rib-to-deck joint is one of the most representative types. At the crossbeam conjunction, high stress concentration makes the joint more sensitive to fatigue loading. In this paper, finite element models are built using software program Abaqus integrated with FRANC3D. The calculated stress at uncracked stage is validated with measured data obtained from laboratory tests. Afterwards, cracks are inserted at the weld root and the stress intensity factor ranges in mode I (ΔK_I) are calculated. Parametric analysis with various cracks is carried out. General correction factors are calculated from the finite element calcualtion with the power fit values.

Peer-review under responsibility of the ECF22 organizers.

Keywords: OSDs, rib-to-deck joint, weld root crack, stress intensity factors;

1. Introduction

Orthotropic steel deck is a common type of deck plates used in the steel bridges. The component uses welding technique to connect steel plates and provides high load capacity in longitudinal direction with low self-weight (7) and (5). During the 70 years of application, the deck plates have been sucessfully used in the long span bridges and movable bridges. However, the all welded component is prone to fatigue loading. Under the heavy truck loading, cracks appear at various positions of the decks, mainly in the welded joints. Among them, the rib-to-deck crack at the crossbeam conjucntion is one the most representative types, see Fig. 1. Cracks 1 and 2 (C1 and 2) initiates from the weld root of the stiffeners and grow in the deck plate. Compared with the C2, the stress concentration at C1 is higher due to the existance of crossbeam. Because of the high inspection and repair cost for this kind of crack, it is important to avoid or control the crack within its service life.

In recent years, the newly designed OSDs trend to use thicker deck plates and improved welding techniques which affect its fatigue performance. A research programme is therefore started in the Netherlands to study the fatigue

* Corresponding author. Tel.: +31-152784752.
E-mail address: W.Wu-1@tudelft.nl

2452-3216
Peer-review under responsibility of the ECF22 organizers.
10.1016/j.prostr.2018.12.214

behaviour of the new OSDs. Full-scale fatigue tesing and numerical modelling is included in the programme. The testing part of the rib-to-deck joint at crossbeam conjunction is reported in the reference (11). The relationship of total fatigue life and coresponding stress ranges is provided from the testing. It is known that the marcocrack propagation period dominates the fatigue behaviour of welded joints. By using fracture mechanics approach, the whole process in the crack propagation period can be studided. In recent years, the method has been sucessfully used for the fatigue life assessment of steel structures (1) and (8).

In this paper, an advanced finite element model is built containing the cracks using software Abaqus 6.14-1 (10) integrated with FRANC3D 7.1 (4). The stress intensity factors are calcualted within the frame of linear elastic fracture mechanics based on M-integrity (4). Through parametric analysis, the best fit curves of general correction factors are found. The data can be used for the hand calcualtion following the weight function procedure (2).

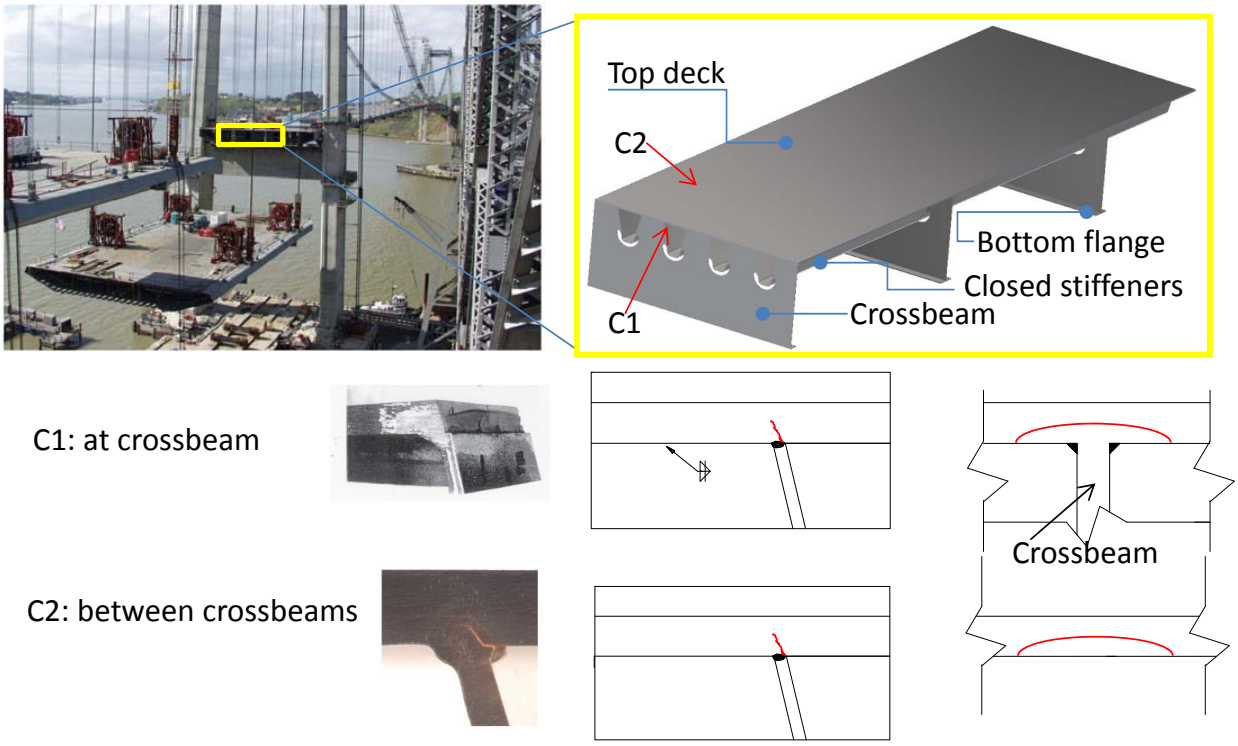

Fig. 1. Sketch of rib-to-deck joint at crossbeam conjunciton (3), (7)

2. Finite element models

2.1. Loading and boundary condition

An advanced finite element model is built following the testing specimen and loading set-ups in reference (11). In Fig. 2, the load range of 144 kN with ratio of 0.1 is applied from the top of the steel plate to simulate the loading situation of Stiffener 7 in reference (11). It is found that the stress situation of the rib-to-deck joint is mostly affected by the closest 2 stiffeners (5). In the model, the bottom flange is fixed on the ground. Sysmetric conditions are applied at the sides.

2.2. Geometric information and interaction properties

In Fig. 2, the 3 trapezoid stiffeners support the 20 mm thick top deck (represented by t in the following sections). The crossbeam is 968 mm high with “Haibach” cutout at the bottom of stiffeners. Sub models A and B are created

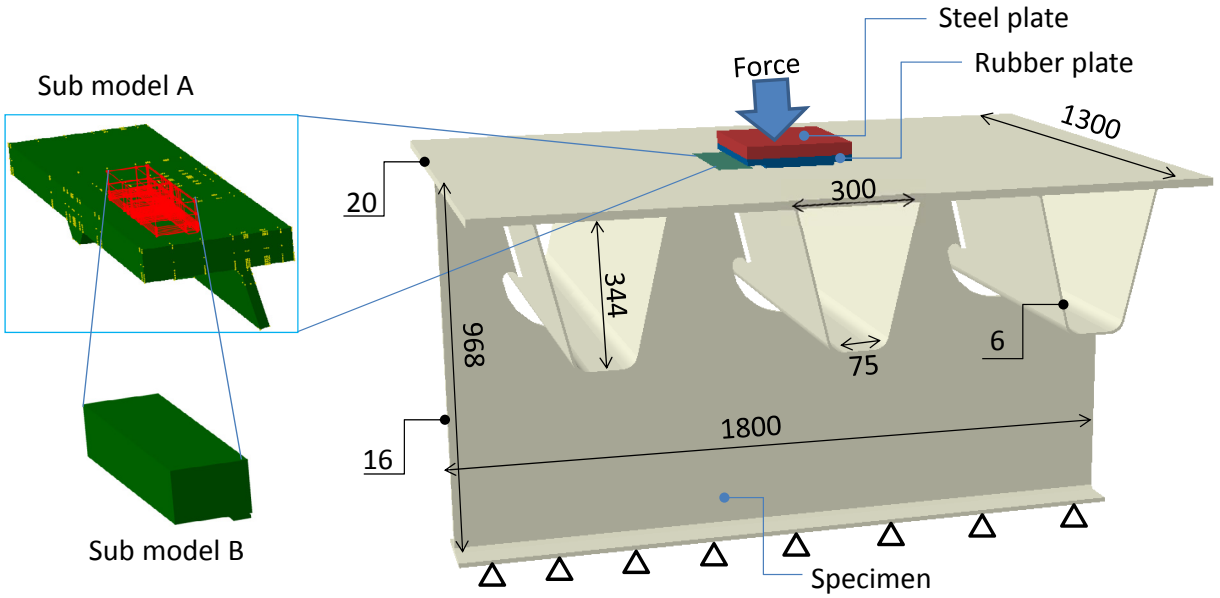

Fig. 2. Sketch of the FE model (unit:mm)

with “tie” constraints at the intersect faces. In this way, the area of interest can be refine meshed while keeping the remaining area coarse meshed. At the center of top deck, the contact behaviour of the 180 mm×320 mm rubber plate and steel plate is considered with “hard” contact in normal direction and “penatly” function in tangential direction with friction coefficient 0.3 (10). Above it, the “tie” constraint is applied at the intersection of steel and rubber plates.

2.3. Crack insert

In the model different sizes and shapes of the crack is inserted in the weld root of the joint, see Figs. 3 and 4. As observed from the previous testing, it is found that the angle between the crack and the vertical line is around 30° which is used when inserting the cracks in the model. In general, the cracks are described as semi-ellipse shape with half depth a (with d in the deck thickness direction) and half length c. ΔK_I at 3 positions are considered (P1 at the edge, P2 at the deepest point, and P3 at the middle point of edge and deepest point) with various sizes and shapes of the crack.

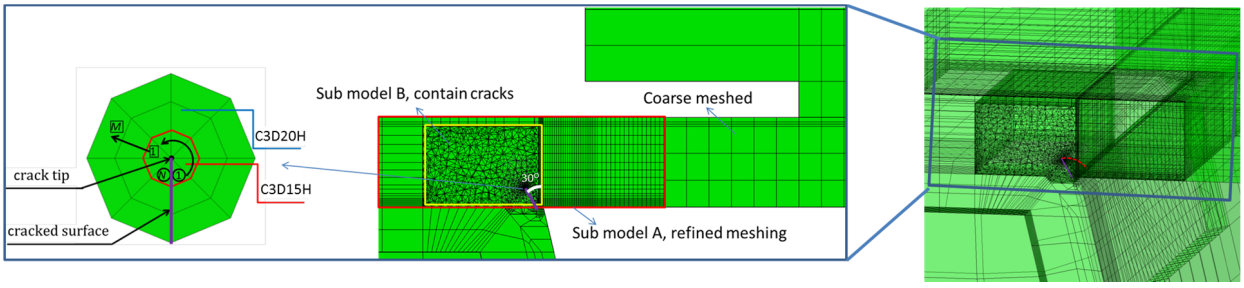

Fig. 3. Crack and meshing of the FE model

2.4. Meshing and material properties

In the model, solid element C3D8H is used for the global area and sub model A (10). In sub model B, 3 cirlce element is created around the crack tip with the inner circle with element C3D15H and the outer ones C3D20H (4).

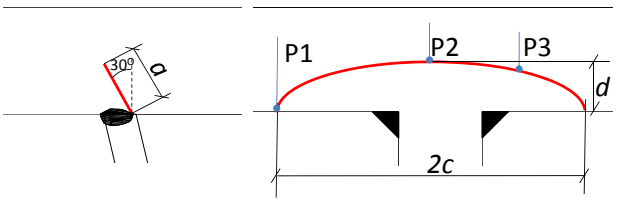

Fig. 4. Shape of the crack in FEM

The remaining element in sub model B is C3D10H. Young's modulus of steel, E_s, is 210 GPa with ν_s 0.3. For the hyperealasitc rubber material, the C_{10} and C_{20} are 0.4613 MPa and 0.0175 MPa, repectively. D_1 and D_2 are 2.5×10^{-5} MPa^{-1} and 2.0×10^{-5} MPa^{-1} (12).

3. Validation of the uncracked model

As mentioned before, the model is built following the testing specimen in the reference (11). One of the tested joint, the north side of Stiffener 7, is selected for the analysis in this paper. A comparison of the measured stress ranges (mutiply the measured strain range with E_s) and FE calculation is shown in Fig. 5. The measured stress ranges are compared with the calculated ones which shows good agreement in both the top and bottom of the deck plate.

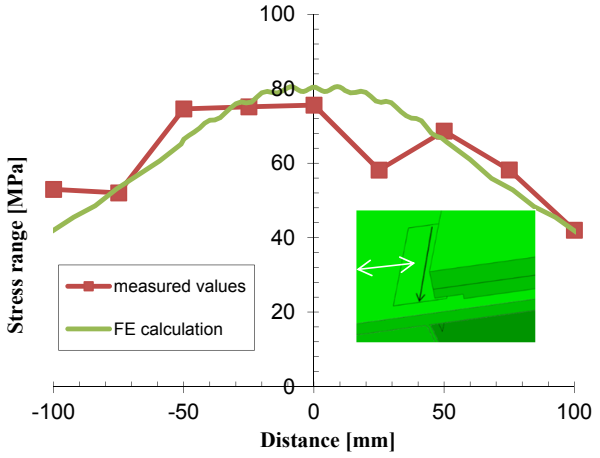

(a) top of the deck, longitudinal direction

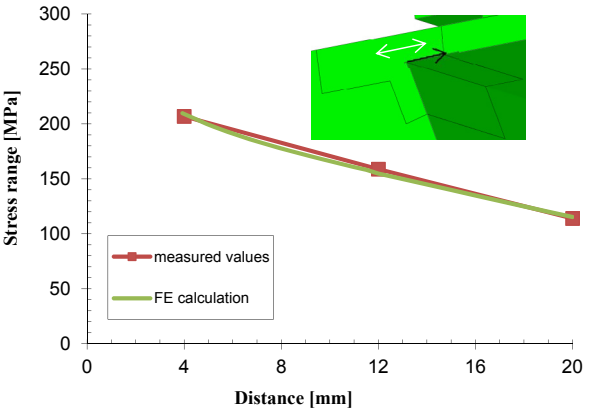

(b) top of the deck, transverse direction

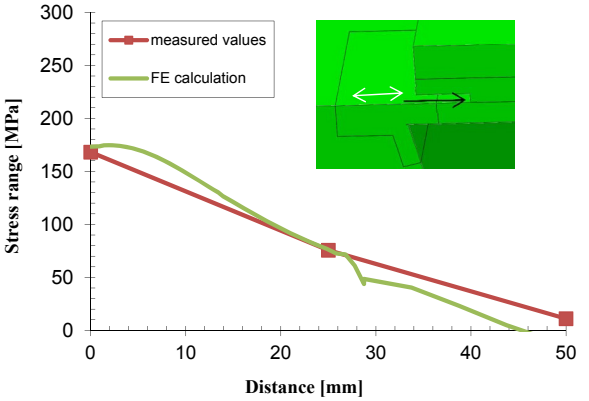

(c) bottom of the deck, transvers direction

Fig. 5. Comparison of the stress distribution in testing and FE calculation

4. Results

4.1. SIFs at the crack tips

In Fig. 6, 4 different sizes of the crack with shape $c/a = 3$ is shown. When the crack is small ($a = 1$ mm) the largest ΔK_{I} locates at relative distance range 0.1-0.9 with value around 750 N/mm$^{3/2}$. With the growth of crack, the values are dropping which ends with 480 N/mm$^{3/2}$ at $a = 15$ mm. In general, ΔK_{I} distributes evenly in the middle area (relative distance 0.3-0.7) along the crack length and decrease with the crack growth. Detailed change of ΔK_{I} at P2 can be found in Fig. 7. This finding is in a line with the ΔK_{I} in Fig.6.

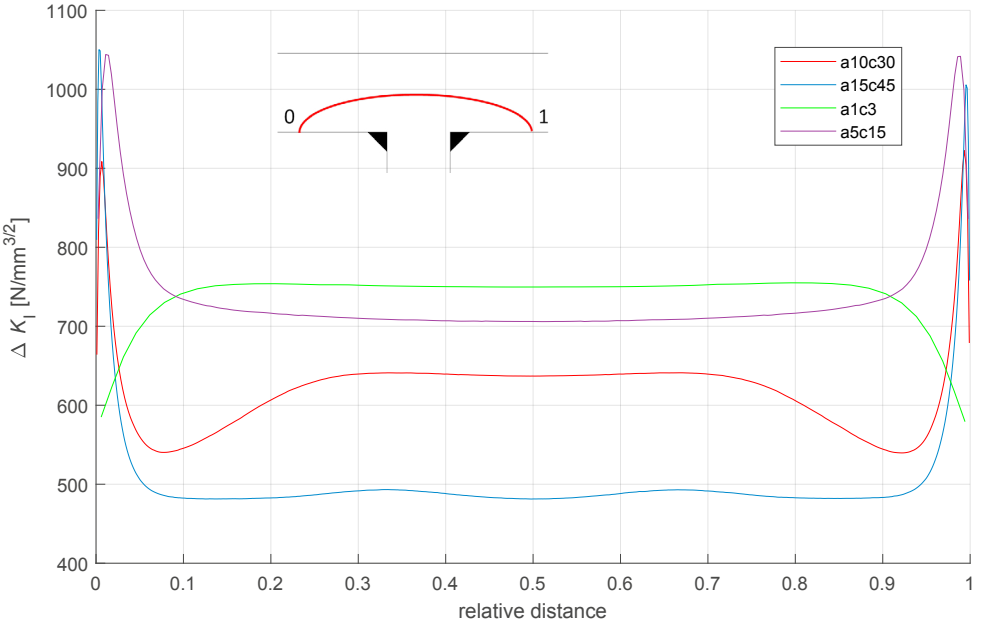

Fig. 6. ΔK_{I} along crack tip in the case c/a=3

4.2. Effect of crack shapes

Three different cases, *c/a*= 1, 3, and 5, are considered for the effect of the crack shapes on the ΔK_{I} at P2. In Fig. 7, ΔK_{I} decreases almost linearly with the d/t in case $c/a = 1$. When the crack is more shallow, with *c/a*= 3 and 5, the change of the ΔK_{I} is much more gentle and almost stable when $d/t < 0.4$. Afterwards a linear change is observered. This indicates the constant propagation speed at the early stage of shallow cracks. In the later stage, the speed drops due to the change of structural integrity at the cracked area which is in a line of the observed strain range redistribution reported in reference (11).

4.3. General correction factors

In the crack propagation analysis using weight function approach, ΔK_{I} is calculated by equation (1). The accurate general correction function $Y(\frac{d}{t})$ is important for the propagation analysis. For this joint, limited information is provided to caculate the weight founction and there is no formula for the newly designed deck with 20 mm thick deck plate. In Fig. 8, $Y(\frac{d}{t})$ at P2 of different sizes (d/t) and shapes (a/c) of the crack is shown with the best fit equations. Hot spot stress ranges $\Delta\sigma_{HSS}$ is 226 MPa, calculated by the surface extrapolation using data in Fig. 5c. The crack depth at its component in the deck thicness direction d is used in calculation $Y(\frac{d}{t})$. The power function relationship is found in all 3 cases with varibles shown in the legend of Fig. 8. The general functions in *c/a*=1.0 and 3.0 distribute

quite close which indicate that the propagation speeds are close at the deepest position for these cases. It should be noticed that the sigularity exists with d/t is close to 0. More calculation needs to be carried out when the crack is small.

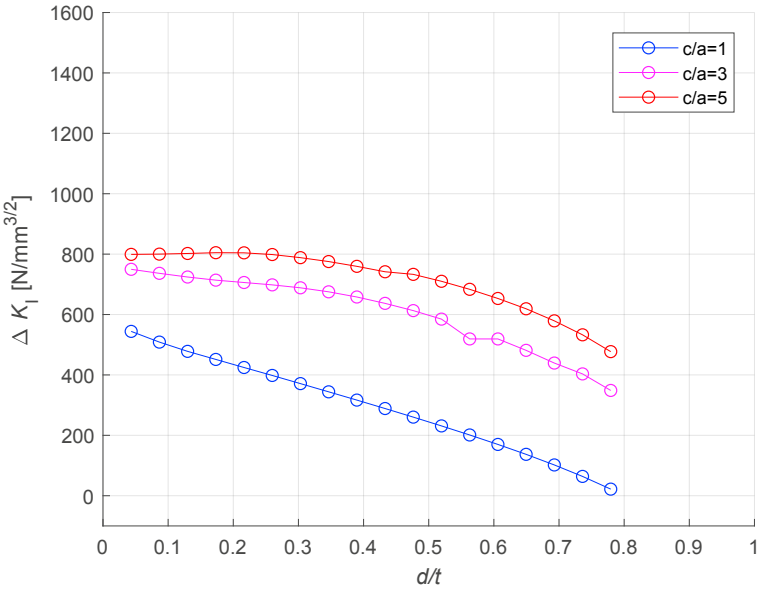

Fig. 7. ΔK_I at P2 with c/a=1, 3, and 5

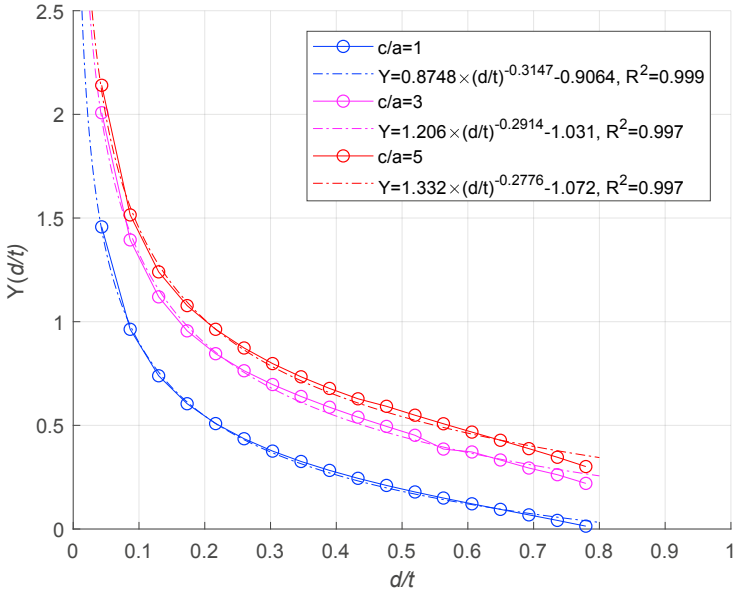

Fig. 8. General correction function at P2 with c/a=1, 3, and 5

$$\Delta K = Y(\frac{d}{t}) \cdot \Delta\sigma_{HSS} \cdot \sqrt{\pi \cdot d} \tag{1}$$

5. Conclusions

Cracks initiates at the weld root of the rib-to-deck joint at crossbeam conjunction in OSDs is numerically studied in this paper. Advanced finite element models with different shapes of cracks are built to calculate the ΔK_{I} and $Y(\frac{d}{t})$ at different stages. The following conclusions can be drawn:

- In case $c/a = 3$, ΔK_{I} distributes evenly in the middle area (relative distance 0.3-0.7) along the crack length and decrease with the crack growth.
- In case $c/a = 1$, a linear decrease trend of ΔK_{I} is found at the deepest point with crack growth. For more shallow cracks, $c/a = 3$ and 5, ΔK_{I} is stable when $d/t < 0.4$.
- The general correction function $Y(\frac{d}{t})$ for the deepest points shows a power relationship with the relative crack depth d/t. Close value is found in the cases $c/a = 3$ and 5.

Acknowledgements

The first author would like to thank the financial support from China Scholarship Council (CSC) for the PhD study.

References

[1] Aygül, M.,2013. *Fatigue evaluation of welded details–using the finite element method*. PhD thesis, Chalmers University of Technology.
[2] BSI.,2016. *BS 7910:2013+A1:2015. Guide to methods for assessing the acceptability of flaws in metallic structures*. British Standard Institution.
[3] Connor,R., Fisher,J.,2012. *Manual for design, construction, and maintenance of orthotropic steel deck bridges*. FHWA report.
[4] Fracture Analysis Consultants.,2017. *FRANC3D V7.1 ABAQUS Tutorial*. Fracture Analysis Consultants.
[5] de Jong,F.B.P.,2007. *Renovation techniques for fatigue cracked orthotropic steel bridge decks*. PhD thesis, TU Delft, Delft University of Technology.
[6] Hobbacher,A.,2016. *Recommendations for fatigue design of welded joints and components*. Springer International Publishing.
[7] Kolstein,M.H.,2007 *Fatigue classification of welded joints in orthotropic steel bridge decks*. PhD thesis, TU Delft, Delft University of Technology.
[8] Nagy,W.,2017. *Fatigue assessment of orthotropic steel decks based on fracture mechanics*. PhD thesis, Ghent University.
[9] Pachoud,AJ.,Manso.PA, and Schleiss,AJ. Stress intensity factors for axial semi-elliptical surface cracks and embedded elliptical cracks at longitudinal butt welded joints of steel-lined pressure tunnels and shafts considering weld shape. *Engineering Fracture Mechanics*, 179:93–119, 2017.
[10] Simulia.,2014. *ABAQUS analysis user's Manual, Version 6.14*. Simulia.
[11] Wu,W., Kolstein,M.H., Veljkovi,M., Pijpers,R., and Vorstenbosch-Krabbe,J.,2017. 09.04: Fatigue behaviour of the closed rib to deck and crossbeam joint in a newly designed orthotropic bridge deck. *Eurosteel2017*, 1(2-3):2378–2387.
[12] Xu,X.,Liu,Y.,He,J.,2014. Study on mechanical behavior of rubber-sleeved studs for steel and concrete composite structures. *Construction and Building Materials*, 53:533 – 546.